Hysteretic current–voltage characteristics in RF-sputtered nanocrystalline TiO$_2$ thin films

Manuel Villafuerte[a,b,*], Gabriel Juárez[a], Silvia P. de Heluani[a], David Comedi[a,b]

[a]Laboratorio de Física del Sólido, Facultad de Ciencias Exactas y Tecnología, Universidad Nacional de Tucumán,
Av. Independencia 1800, San Miguel de Tucumán 4000, Argentina
[b]Consejo Nacional de Investigaciones Científicas y Técnicas (CONICET), Argentina

Abstract

We have measured the current–voltage characteristics at room temperature of a nanocrystalline TiO$_2$ thin film fabricated by reactive RF-sputtering deposition and sandwiched between ITO (indium–tin–oxide)-buffered glass substrate and an indium top electrode. The I–V characteristics are ohmic for low voltages and become non-linear, hysteretic and asymmetric as the voltage is increased. The system is shown to be well represented by two distinct resistance states in the non-ohmic region. Current transient evolutions were also measured for constant voltage excitations. The resistance is stable in time for voltages in the ohmic regime. In contrast, for voltages in the non-ohmic regime, the resistance has a small variation for a short period of time (order of tens seconds) and then increases with time. For those transients, long characteristic times (on the order of tens of minutes up to hours) were found. The behavior of the system is discussed on the basis of experimental results reported in the literature for similar systems and existing models for electric-field induced resistive switching.
© 2007 Elsevier B.V. All rights reserved.

1. Introduction

Resistive switching in transition metal oxide films, such as TiO$_2$, attracts great interest for a possible application in non-volatile memory devices due to low current required for switching, compared with phase change memories [1]. Resistance switching and voltage-controlled negative resistance phenomena have been observed since the 1960s on materials such as amorphous semiconductors [2–4] and ZnSe–Ge heterostructures [5], as well as on a variety of oxides such as Nb$_2$O$_5$ [6], Al$_2$O$_3$ [7], Ta$_2$O$_5$ [8], TiO$_2$ [9], and NiO [10,11]. An apparently related, but nevertheless new phenomenon, known as Electric Pulse-Induced Resistance switching (EPIR), has been recently reported in Pr$_{0.7}$Ca$_{0.3}$MnO$_3$ thin films at room temperature [12]. In this novel effect, a non-volatile change of the electrical resistance between two electrodes is observed after applying an electric pulse. Thus, the EPIR effect is different from "conventional" resistance switching where the effect is not polarity dependent [13]. Furthermore, the direction of the resistance change (i.e. either increased or decreased resistance) depends on the polarity of the electric pulse in EPIR. Although EPIR has been intensively studied in recent years, its physical origin is still far from being satisfactorily understood. Many different models have been proposed, such as charge trapping in small domains [14], electron accumulation at the electrode-film interface [15], creation of crystalline defects [16], trap-assisted phase separation process at the interface [17], and a filamentary model [18]. In this work, we study the I–V characteristics of In/TiO$_2$/ITO (ITO = indium–tin–oxide) heterostructures and show that it exhibits the hysteretic and asymmetric behavior characteristics of the EPIR change effect.

*Corresponding author. Tel.: +54 381 4364093 x 7770;
fax: +54 381 4363004.

E-mail address: mvillafuerte@herrera.unt.edu.ar (M. Villafuerte).

2. Experimental

The In/TiO$_2$/ITO heterostructure was prepared by depositing the TiO$_2$ on a commercial conducting ITO–coated glass substrate and by soldering small In contacts on the top TiO$_2$ film surface. The TiO$_2$ film had been fabricated by the RF-diode reactive sputtering of a titanium target in an O$_2$ + Ar gas mixture using an O$_2$ flow rate of 0.16 sccm and a substrate temperature of 350 °C. The structure of the TiO$_2$ film is nanocrystalline with crystallite size of about 37 nm, as deduced from X-ray diffraction curves. The two main polymorphs of TiO$_2$, anatase and rutile are present in the film with estimated volume ratio of 5.5 (anatase/rutile). Rutherford back-scattering measurements reveal that the film is actually slightly above stoichiometry with an atomic O/Ti ratio of 2.04 ± 0.02 [19]. The TiO$_2$ film thickness is 400 nm.

Copper wires were indium-soldered on the top surface of the film and on the ITO bottom electrode for electrical measurements. The schematic diagram showing sample contacting and electrical connections used is shown in the inset of Fig. 1. The positive bias was defined by the current flowing from the top In electrode to the bottom ITO electrode.

3. Results and discussions

Fig. 1 shows an I–V curve of the In/TiO$_2$/ITO heterostructure at room temperature in vacuum (pressure ⩽ 1 mTorr) under a voltage sweep: 0 → +2 V → 0 → −2 V → 0. Hysteresis and asymmetry phenomena were clearly observed. From Fig. 1 it can be seen that positive voltages switch the resistance to lower values and negative voltages switch to higher values. It is clear that Joule heating cannot produce a hysteresis like the one shown in Fig. 1 for negative bias since TiO$_2$ has semiconductor-like resistance behavior (i.e., heating would yield to a reduction of the resistance, while an opposite effect is observed in this case). Also, it is worth noting that this bipolar switching behavior is different from the unipolar behavior reported in reference [18]. There, heterostructures containing much
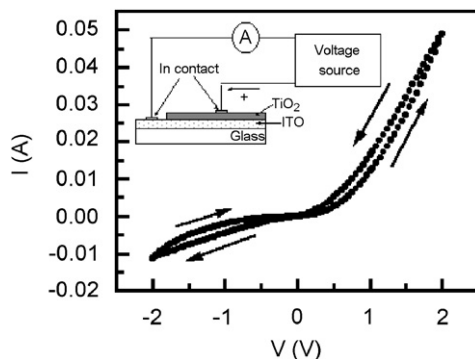
thinner anatase TiO$_2$ films (27 nm) between the electrodes were tested and switching is achieved regardless the polarity of the applied voltages. It is possible that this different behavior could be due to the larger intensity of applied electric fields as compared with those used here. The behavior found here, in contrast, resembles that reported for various perovskite-type oxides (see for instance ref. [13,17]).

Fig. 2 shows a double logarithmic plot of the I–V curves for the positive bias for high resistance states (HRS) and low resistance states (LRS). The IV curves show a slope of 1 and a reversible behavior for voltages lower than ~0.1 V. At higher voltages (~0.1 V–~2 V), the response is non-ohmic and a slight hysteresis is found for both HRS and LRS curves that is not distinguished in Fig. 2. For voltages higher than ~2 V, the system switches to LRS and the I–V curve shows hysteresis.

The inset of Fig. 2 shows the resistance vs. voltage calculated from I–V curves for LRS and HRS under a voltage sweep: +0.05 V → +1 V → +0.05 V. Note that the slight hysteresis for the HRS branch, which is unnoticed in the I–V plot scale of Fig. 2, can be seen in the resistance scale of the inset. The resistance ratio of around 4 for this sample is low compared with previous bibliography (⩾ 100) [20]. In the same reference the authors explore the local conductivity at nanoscale using conductive atomic force microscopy and they found essentially two switching modes: one via filament formation, where resistance ratio of around 1000 was obtained, and other of an area without filaments, where resistance ratio of approximately 5 was obtained.

We argue that we have a heterostructure with just one of those switching modes: switching without filaments. The elements that combine to yield this behavior are: larger thickness, as discussed above; the slightly above stoichiometry that reduces the formation of oxygen vacancies and extended defects, that could form conducting filaments, and also considering that the contact between TiO$_2$ and In, which have a work function of 3.8 eV, is less blocking when
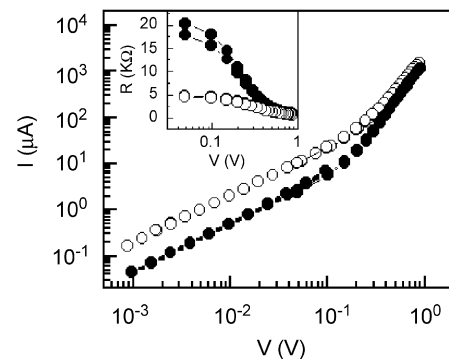

Fig. 1. I–V curve of an In/TiO$_2$/ITO heterostructure at room temperature. The arrows indicate sweeping directions. The inset shows the schematics of the samples and measurements.

Fig. 2. I–V characteristics of an In/TiO$_2$/ITO heterostructure in a double-logarithmic plot for positive bias region. Filled symbols correspond to the HRS and open symbols for LRS. Inset: resistance vs. voltage calculated from I–V curve.

compared with TiO_2 and Pt or Ru (5.5 and 5.1 eV, respectively) used as contacts in the cited reference [20].

In order to investigate the time stability of the current at room temperature we performed current vs. time at constant voltage experiments. For voltages lower than 0.1 V (ohmic region) the current shows no changes for the range of times measured in this work (1000 s); the resistive "state" of the sample is stable in time. However, this is not the case for voltages higher than 0.1 V, i.e. in the non-linear region of the I–V curves. Fig. 3 shows a double logarithmic plot of the time evolution of current for a constant applied voltage of $+0.5$ V for the sample in LRS. The time $t = 0$ corresponds to the instant at which the voltage is applied. After a period of time of the order of tens of seconds without significant changes, the current starts to decrease, indicating an increase in resistance.

It could be argued that such an increase in resistance when the system is in the LRS reveals a decay of this state back to the HRS. However, the resistance increase with time seems to be a characteristic feature of the system whenever it is in the non-linear region of the I–V curve, regardless whether it is in the HRS or in the LRS. Fig. 4 shows a double logarithmic plot of the current as a function of time for a constant applied voltage of $+0.5$ V for the sample in the HRS. It can be seen that the current
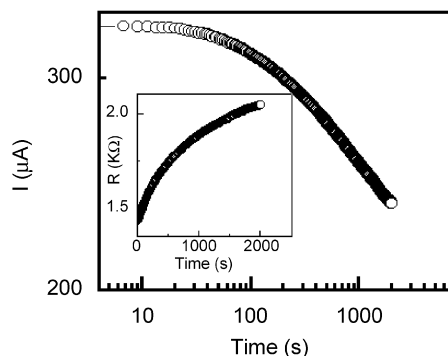
also decays with time, resembling the behavior shown in Fig. 3 for the LRS.

The retention behavior was investigated in [20] in the LRS and HRS at room temperature for several days. They found that HRS increase 5.2 times faster than that of the LRS. They suggest that the conducting filaments of the LRS are more immune to thermal disturbance. From Figs. 3 and 4 it can be observed that there is a similar increase in the rate of resistance of around 1.4 times for 2000 s, for both LRS and HRS. This behavior suggests that the same transport mechanism is conducting the carriers from one electrode to the other in both the LRS and HRS states.

In the measured range the current transient could be fit with a power-law decay. This type of fit can be explained by a model based on Lévy statistics of waiting times [21].

4. Conclusion

We have investigated the current–voltage characteristics of a $In/TiO_2/ITO$ heterostructure at room temperature in vacuum. The I–V characteristics are ohmic for low voltages and become non-linear, hysteretic and asymmetric as the voltage is increased. The I–V curves resemble the behavior reported for various perovskite-type oxides of the bipolar-type switching. The resistance ratio between LRS and HRS was approximately 4. Comparing this result with the conclusions of Ref. [20] we suggest that there is switching without conducting filaments in our sample. Current transient evolutions were also measured for constant voltage excitations. The resistance is stable in time for voltages in the ohmic regime. In contrast, for voltages in the non-ohmic regime, the resistance increases with time with a rate of around 1.4 for both LRS and HRS ($t < 7000$ s and applied voltage of $+0.5$ V). We can conclude that the same transport mechanism is present for both LRS and HRS.

The final conclusion is that in materials like TiO_2 we can simultaneously have two switching mechanisms, one defined as "conventional switching" and the other as EPIR. We suggest that it is possible to control the prevalence of one or the other by tuning the thickness of the film, work function of the contacts and stochiometry of the oxide.

Fig. 3. Time evolution of the current for constant applied voltage of $+0.5$ V. At $t = 0$ the sample was in LRS. Inset: resistance vs. time calculated from I vs. time.
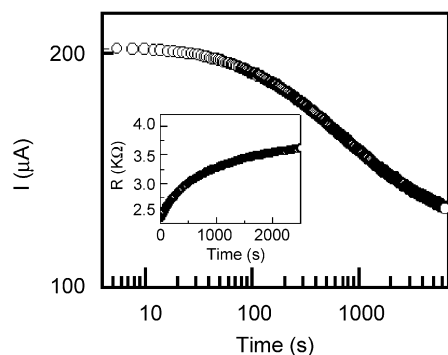

Fig. 4. Time evolution of the current for constant applied voltage of $+0.5$ V. At $t = 0$ the sample was in HRS. Inset: resistance vs. time calculated from I vs. time.

References

[1] C. Rohde, B.J. Choi, D.S. Jeong, S. Choi, J.-S. Zhao, C.S. Hwang, Appl. Phys. Lett. 86 (2005) 262907.
[2] S.R. Ovshinsky, Phys. Rev. Lett. 36 (1968) 1469.
[3] J.F. Dewald, A.D. Pearson, W.R. Northover, W.F. Peck Jr., J. Electrochem. Soc. 109 (1962) 243c.

[4] G. Dearnaley, A.M. Stoneham, D.V. Morgan, Rep. Prog. Phys. 33 (1970) 1129.

[5] H.J. Hovel, J.J. Urgell, J. Appl. Phys. 42 (1971) 5076.

[6] W.R. Hiatt, T.W. Hickmott, Appl. Phys. Lett. 6 (1965) 106.

[7] T.W. Hickmott, J. Vac. Sci. Technol. 6 (1969) 828.

[8] K.L. Chopra, J. Appl. Phys. 36 (1965) 184.

[9] F. Argall, Solid State Electron 11 (1968) 535.

[10] J.F. Gibbons, W.E. Beadle, Solid-State Electron 7 (1964) 785.

[11] J.C. Bruyere, B.K. Chakraverty, Appl. Phys. Lett. 16 (1970) 40.

[12] S.Q. Liu, N.J. Wu, A. Ignatiev, Appl. Phys. Lett. 76 (2000) 2749.

[13] M. Hamaguchi, K. Aoyama, S. Asanuma, Y. Uesu, T. Katsufuji, Appl. Phys. Lett. 88 (2006) 142508.

[14] M.J. Rozenberg, I.H. Inoue, M.J. Sanchez, Phys. Rev. Lett. 92 (2004) 178302.

[15] A. Sawa, T. Fujii, M. Kawasaki, Y. Tokura, Appl. Phtys. Lett. 85 (2004) 4073.

[16] A. Baikalov, Y.Q. Wang, B. Shen, B. Lorenz, S. Tsui, Y.Y. Sun, Y.Y. Xue, C.W. Chu, Appl. Phys. Lett. 83 (2003) 957.

[17] D.S. Shang, Q. Wang, L.D. Chen, R. Dong, X.M. Li, W.Q. Zhang, Phys. Rev. B 73 (2006) 245427.

[18] D.S. Jeong, H. Schroeder, R. Waser, Appl. Phys. Lett 89 (2006) 082909.

[19] D. Comedi, M. Villafuerte, G. Juarez, S.P. Heluani, ECS Trans. 3(11) 135 (2006).

[20] B.J. Choi, D.S. Jeong, S.K. Kim, C. Rohde, S. Choi, J.H. Oh, H.J. Kim, C.S. Hwang, K. Szot, R. Waser, B. Reichenberg, S. Tiedke, J. Appl. Phys. 98 (2005) 033715.

[21] D.S. Novikov, M. Drndic, L.S. Levitov, M.A. Kastner, M.V. Jarosz, M.G. Bawendi, Phys. Rev. B 72 (2005) 075309.